Dynamical model for correlated two-pion exchange in the NN interaction

H.-C. Kim,* J.W. Durso,† and K. Holinde
Institut fur Kernphysik IKP(Theory), Forschungszentrum Jülich GmbH, D-52425 Jülich, Germany
(Received 15 October 1993)

A dynamical model for S- and P-wave correlated two-pion exchange between two nucleons is presented, starting from corresponding $N\bar{N} \to \pi\pi$ amplitudes in the pseudophysical region, which have been constructed from nucleon and Δ-isobar exchange Born terms and a meson exchange model of $\pi\pi$ scattering which satisfactorily describes the empirical $\pi\pi$ data. It is demonstrated that the results have quite different characteristics, in both strength and range, compared to (sharp mass) σ', ρ exchange as used in the Bonn potential. Consequences for the description of high partial wave NN scattering phase shifts are discussed.

PACS number(s): 13.75.Cs, 21.30.+y

I. INTRODUCTION

Since Yukawa [1] proposed that the strong interaction between two nucleons is mediated by the exchange of mesons in analogy with photon exchange in quantum electrodynamics, the meson theory of nuclear forces has been vigorously pursued in order to describe the nucleon-nucleon (NN) interaction both qualitatively and quantitatively. Indeed, even nowadays this picture is fully justified: Although quantum chromodynamics (QCD), with quarks and gluons as fundamental degrees of freedom, is believed to be the underlying theory of the strong interaction, baryons and mesons have definitely retained their importance as relevant degrees of freedom for a realistic description of low energy nuclear phenomena.

There are numerous examples of successful NN potentials based on meson exchange. After the experimental discovery of vector mesons in the early 1960s, simple one-boson exchange (OBE) models have been constructed (see, e.g., Refs. [2–4]) which, despite the use of very few parameters, were able to account reasonably well for the empirical NN data below pion production threshold. However, conceptually such models are not satisfactory. Their main deficiency is the use of a fictitious scalar-isoscalar boson, $\sigma_{\rm OBE}$ (with a mass around 500 MeV), which does not exist but is needed to provide the intermediate-range attraction. Indeed it should be viewed as a mere—and quite rough— parametrization of 2π-exchange processes in the $J^P = 0^+$ state of the t channel. A realistic inclusion of such 2π-exchange contributions (which replace not only the σ but also the ρ meson of OBE models) can be done with the help of dispersion relations using πN and $\pi\pi$ data. Corresponding NN potentials were developed in the 1970s, in particular by the Stony Brook [5,6] and Paris [7–9] groups.

Although the dispersion theoretical approach, which obtains the 2π-exchange interaction from empirical data, is certainly adequate for free NN scattering, it is insufficient when dealing with the many-nucleon system. For example, modification of the interaction in the nuclear medium cannot be taken into account in a well-defined way. The study of such effects requires an explicit field theoretical description, including the Δ, isobar in intermediate states, which is also essential for a consistent evaluation of pion production processes, three-body forces and meson exchange currents.

The (full) Bonn potential [10] contains, apart from single-meson exchanges (π, ω, δ), uncorrelated 2π-exchange processes with NN, $N\Delta$, and $\Delta\Delta$ intermediate states, see Fig. 1. Corresponding correlated processes (for $J^P = 0^+$ and 1^- in the t channel) are included in a simplified way, parametrizing them by simple σ' and ρ exchange with a sharp mass of 550 and 769 MeV, respectively (see Fig. 2). Diagrams analogous to Fig. 1 involving heavy mesons are included too, especially the contributions with π and ρ, which prove to be of outstanding importance. (Note, however, that corresponding correlated contributions are missing.) It is important

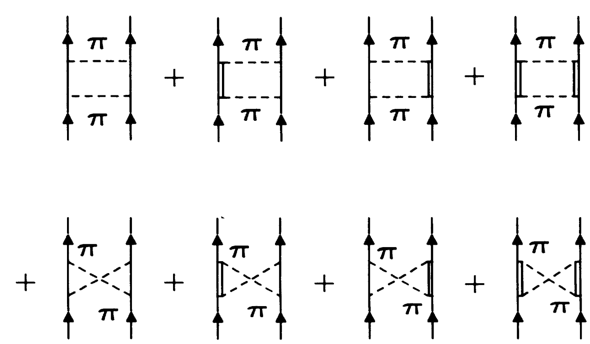

FIG. 1. Uncorrelated 2π-exchange contributions as used in the Bonn NN potential [10]. The double line denotes the Δ isobar.

*Present address: Institut für Theoretische Physik II, Ruhr-Universität Bochum, 44780 Bochum, Germany.

†Permanent address: Department of Physics, Mount Holyoke College, Holyoke MA 01075-1461.

to realize that this σ' of the Bonn potential is not to be viewed as a genuine particle but this exchange (as well as ρ exchange) merely serves as a simple parametrization of correlated 2π-exchange processes. As such, however, it is subject to the same criticism brought up against the dispersion theoretical approach before: While possibly adequate for free NN scattering, medium modifications (e.g., change of the intermediate pions) cannot be considered. This is especially serious since, as shown, e.g., by Durso *et al.* [11], the correlated processes of Fig. 2 provide by far the dominant contributions compared to the uncorrelated processes of Fig. 1. Consequently, the goal of providing an explicit NN interaction model adequate for the use in the nuclear environment has only partially been realized in the Bonn model [10].

The aim of the present work is to provide such an explicit model for the correlated 2π-exchange processes of Fig. 2. This requires as input a realistic $\pi\pi$ T matrix, which, in this work, is generated from a potential model $V_{\pi\pi}$ developed by our group some years ago [12]. It is likewise based on meson exchange and involves the coupled channels $\pi\pi$ and $K\bar{K}$. Corresponding diagrams for $V_{\pi\pi}$ are shown in Fig. 3; empirical $\pi\pi$ phase shifts are well reproduced (cf. Ref. [12]).

The reason for choosing a dynamical model for the $\pi\pi$ interaction instead of a purely phenomenological treatment, as done in Ref. [11], should be obvious: In this way, medium modifications in the diagrams of Fig. 2 can be taken into account not only for the pion legs but also in the interaction itself. Indeed, if the ρ mass in the medium drops [13], the resulting $\pi\pi$ T matrix will be strongly influenced. These changes occur both in the scalar ($J^P = 0^+$) and vector ($J^P = 1^-$) channel since, according to Fig. 3, ρ exchange is included not only in the s, but also in the t channel.

In principle, one could evaluate the processes of Fig. 2 directly in the s ($NN \to NN$) channel. Since our $\pi\pi$ amplitude, generated by a potential model, is by construction not completely crossing symmetric, such a calculation would not necessarily provide a correct representation of the NN amplitude in the t ($N\bar{N} \to N\bar{N}$) channel,

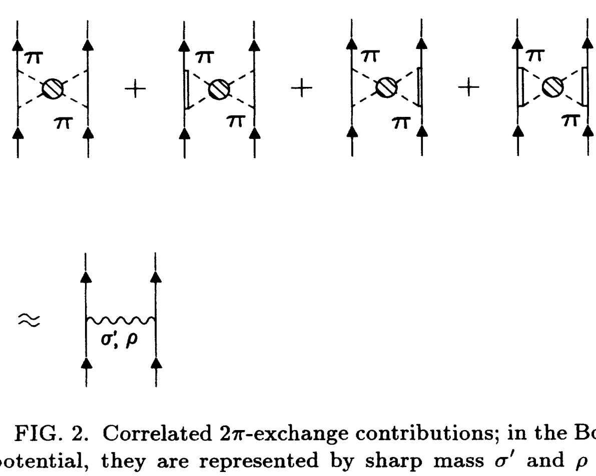

FIG. 2. Correlated 2π-exchange contributions; in the Bonn potential, they are represented by sharp mass σ' and ρ exchange.

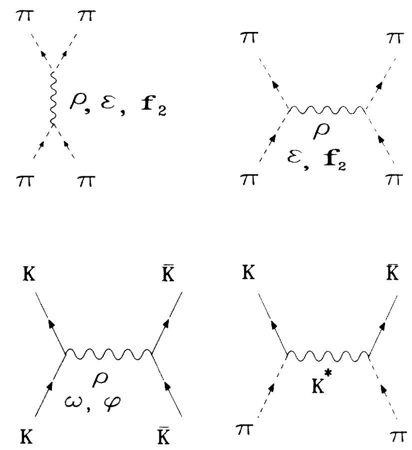

FIG. 3. Meson exchange diagrams used in the $\pi\pi$ interaction model of Lohse *et al.* [12].

which is essential for an adequate description of its range. On the other hand, since we restrict ourselves to rather low energies in the s channel, i.e., to NN scattering below pion production threshold, a correct representation of the s dependence would be of much less significance.

Therefore, we concentrate on the t channel and proceed as in Ref. [11]: First, we evaluate the $N\bar{N} \to \pi\pi$ amplitudes, for $J^P = 0^+$ ("σ") and 1^- ("ρ") in the pseudophysical region $t > 4m_\pi^2$, t being the c.m. energy squared of the $\pi\pi$ system. It is important that these amplitudes can be checked against quasiempirical amplitudes obtained by analytic continuation of πN and $\pi\pi$ data [14]. Finally, a dispersion integral and unitarity together with appropriate subtractions is used to obtain the correlated 2π-exchange contribution to the NN interaction.

As outlined before, our principal motivation for constructing an explicit dynamical model for correlated 2π exchange has been to open up the possibility for a well-defined study of medium effects. In fact, some corresponding results have already been published [15]. Nevertheless, quite interesting results occur already in free NN scattering, which will be addressed in the present paper. Namely, it turns out that the correlated 2π exchange has quite different characteristics compared to σ' and ρ exchange as used in the Bonn potential [10]. Not only is the range different, especially in the scalar channel, which one might have anticipated if a broad mass distribution is replaced by a sharp mass. In fact, the strength provided by the explicit model is also considerably stronger in both the scalar ("σ") and vector ("ρ") channels. We will discuss the consequences for the high partial wave NN scattering phase shifts, and possible implications for the ongoing discussion about the value of the πNN coupling constant.

The outline of the paper is as follows. In the next section, we sketch the basic formalism for obtaining the 2π-exchange contribution to the NN interaction from (pseudophysical) $N\bar{N} \to \pi\pi$ scattering and develop our dynamical model for the S- and P-wave contribution of the latter amplitude. In Sec. III, we present corresponding results and perform a detailed comparison with σ'

and ρ exchange as used in the Bonn potential [10]. The final section contains a short summary and outlook.

II. FORMALISM

In the following we briefly sketch the extensive formalism, which is used to evaluate the 2π-exchange contribution to the NN interaction. For more details we refer the reader to Ref. [16].

A. Dispersion relation for the $NN \to NN$ amplitude

The field theoretical (on-shell) scattering amplitude T is conventionally related to the standard S matrix by

$$S_{fi} = \delta_{fi} - i(2\pi)^4\delta^{(4)}(P_f - P_i)N_f^{-1/2}N_i^{-1/2}T_{fi}, \quad (1)$$

where P_i (P_f) is the total four-momentum in the initial (final) state,

$$N_{i,f} = \prod_{j=1}^{n_{i,f}} 2E_j\Omega/(2m_j)^{b_j}. \quad (2)$$

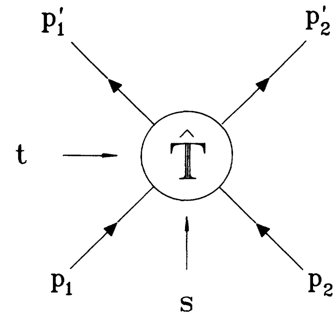

FIG. 4. Diagram visualizing the NN scattering process, in the s ($NN \to NN$) and t ($N\bar{N} \to N\bar{N}$) channels.

Here, $n_{i,f}$ is the number of particles in the corresponding state; each particle has mass m_j, momentum and energy $E_j = (p_j^2 + m_j^2)^{1/2}$; $b_j = 0$ (1) for bosons (fermions) and Ω is the quantization volume. For the s-channel ($NN \to NN$) reaction, cf. Fig. 4, and choosing $\Omega = (2\pi)^3$, Eq. (1) becomes

$$S_{fi} = \delta_{fi} - i(2\pi)^{-2}\delta^{(4)}(p_1' + p_2' - p_1 - p_2)\left(\frac{m_N^4}{E_1'E_2'E_1E_2}\right)^{1/2} T_{fi}. \quad (3)$$

The direct (i.e., s channel) amplitude can be written as

$$T_s(p_1', p_2'; p_1, p_2) = \bar{u}(p_1', \lambda_1')\xi^\dagger(\mu_1')\bar{u}(p_2', \lambda_2')\xi^\dagger(\mu_2')\hat{T}u(p_1, \lambda_1)\xi(\mu_1)u(p_2, \lambda_2)\xi(\mu_2), \quad (4)$$

where $u(k, \lambda)$ is a Dirac helicity spinor normalized to $\bar{u}u = 1$ and $\xi(\mu)$ a Pauli isospinor. The spin and isospin dependence is suppressed on the left-hand side of Eq. (4). For on-shell scattering, the operator $\hat{T}$ can be expressed as a linear combination of 10 invariant operators $\hat{C}_j$ (including isospin); the expansion coefficients c_j are scalar functions of the Mandelstam variables $s \equiv (p_1 + p_2)^2$ and $t \equiv (p_1' - p_1)^2$. (u is not independent but given by $u = 4m_N^2 - s - t$.) $\hat{T}$ can then be written as

$$\hat{T} = \sum_{j=1}^{10} c_j(t, s)\hat{C}_j \quad (5)$$

with $\hat{C}_j$ being a complete set of operators acting in spin and isospin space, i.e., between the Dirac spinors and Pauli isospinors of Eq. (4).

Correspondingly, the amplitude for the t-channel ($N\bar{N} \to N\bar{N}$) process defined in Fig. 4 then reads

$$T_t(-p_1', p_2'; p_1, -p_2) = \bar{v}(-p_1', \bar{\lambda}_{1'})\bar{\xi}^\dagger(\bar{\mu}_{1'})\bar{u}(p_2', \lambda_2')\xi^\dagger(\mu_{2'})\hat{T}u(p_1, \lambda_1)\xi(\mu_1)v(-p_2, \bar{\lambda}_2)\bar{\xi}(\bar{\mu}_2). \quad (6)$$

Here $v(k, \bar{\lambda})$ [$\bar{\xi}(\bar{\mu})$] is the Dirac spinor (isospinor) for an antiparticle. The essential point is that, due to crossing symmetry, $\hat{T}$ can now be represented in the same way as before [Eq. (5)], with precisely the same functions c_j, however in a different s, t domain obtained by replacing p_1' by $-p_1'$ and p_2 by $-p_2$.

According to the Mandelstam hypothesis the analytic properties of the full amplitude leads, for the general case, to a double dispersion relation for the c_j. If one of the variables s, t, u is held fixed, one can derive a one-dimensional dispersion relation containing pole terms and integrals (branch cuts) involving the other two variables.

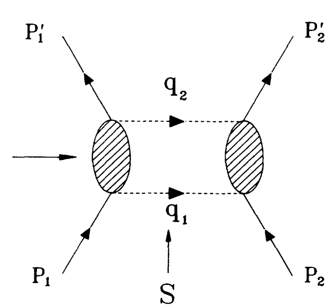

FIG. 5. Diagram visualizing the 2π-exchange contribution to the NN interaction.

Since in this work we are only interested in the 2π-exchange contribution, $T_s^{2\pi}$, and since it is sufficient to consider only the direct term, the corresponding c_j fulfill the following dispersion relation:

$$c_j(t,s) \;=\; \frac{1}{\pi}\int_{4m_\pi^2}^{\infty}\frac{\mathrm{Im}c_j(t',s)}{t'-t-i\epsilon}dt'. \qquad (7)$$

Thus the c_j (and consequently the 2π-exchange amplitude in the s channel) can be determined if this imaginary part is known in the pseudophysical region ($t' \geq 4m_\pi^2$) of the t-channel reaction and for $s \geq 4m_N^2$. This information is now obtained by exploiting the unitarity property of the t-channel amplitude.

B. Unitarity and the $N\bar{N} \to 2\pi$ amplitude

Unitarity relates $\mathrm{Im}T_t^{2\pi}$ [Eq. (6)] to the on-shell $N\bar{N} \to 2\pi$ amplitude (cf. Fig. 5)

$$\mathrm{Im}T_t^{2\pi} \;=\; -\frac{1}{2(2\pi)^2t'}\sum_{\pi\pi}\langle N\bar{N}\mid T^\dagger\mid\pi\pi\rangle\langle\pi\pi\mid T\mid N\bar{N}\rangle\delta^{(4)}(q_1+q_2+p_1'-p_1). \qquad (8)$$

The latter amplitude is defined according to Eq. (1), i.e.,

$$S_{fi} \;=\; -i(2\pi)^{-2}\delta^{(4)}(q_1+q_2+p_1'-p_1)\left(\frac{m_N^2}{E_1'E_1'2\omega_1 2\omega_2}\right)^{1/2}\langle\pi\pi\mid T\mid N\bar{N}\rangle \qquad (9)$$

with $\omega_i \equiv (q_i^2+m_\pi^2)^{1/2}$, and can be represented in the following way:

$$\langle\pi\pi\mid T\mid N\bar{N}\rangle \;=\; \bar{v}(-p_1',\bar{\lambda}_{1'})\xi^\dagger(\bar{\mu}_{1'})\zeta^\dagger(\beta)\hat{T}_{\pi N}\xi(\mu_1)\zeta(\alpha)u(p_1,\lambda_1) \qquad (10)$$

with

$$\hat{T}_{\pi N} \;=\; \hat{T}_{\pi N}^{(+)} - \hat{T}_{\pi N}^{(-)}\boldsymbol{\tau}\cdot\mathbf{t}, \qquad (11)$$

$\mathbf{t}$ ($\boldsymbol{\tau}$) being the isospin operator for the pion (nucleon), and

$$\hat{T}_{\pi N}^{(\pm)} \;=\; -\left[A^{(\pm)}(t,s_t) \;+\; B^{(\pm)}(t,s_t)\gamma\cdot Q\right]. \qquad (12)$$

Here, $Q \equiv \frac{1}{2}(q_2-q_1)$, $t=(p_1-p_1')^2$, and $s_t=(p_1-q_1)^2$. In the c.m. system of the $N\bar{N}$ reaction, $Q=(0,-\mathbf{q})$, $t=4E_p^2=4\omega_q^2$, and $s_t \;=\; -(\mathbf{p}^2+\mathbf{q}^2-2pqx)$, with $\mathbf{p}=\mathbf{p}_1, \mathbf{q}=\mathbf{q}_1$, and $x=\cos\theta_t$, where θ_t is the scattering angle between $\mathbf{q}_1$ and $\mathbf{p}_1$ in the t channel. Since we only want to include the 2π-exchange contribution in the scalar ($J^P=0^+$) and vector ($J^P=1^-$) channels, we have to perform a partial wave expansion for both $A^{(\pm)}$, $B^{(\pm)}$

$$A^{(\pm)}(t,x) \;=\; \sum_J\left(J+\frac{1}{2}\right)A_J^{(\pm)}(t)P_J(x) \qquad (13)$$

and the same for $B^{(\pm)}$. In order to have amplitudes free of kinematical singularities, new helicity amplitudes $f_\pm^{J\,(\pm)}$ are introduced [17]

$$f_+^{J\,(\pm)} = \frac{1}{8\pi}\left[-\frac{p^2}{(pq)^J}A_J^{(\pm)} \;+\; \frac{m_N}{(2J\;+\;1)(pq)^{J-1}}\left\{(2J\;+\;1)B_{J+1}^{(\pm)} \;+\; JB_{J-1}^{(\pm)}\right\}\right],$$

$$f_-^{J\,(\pm)} = \frac{1}{8\pi}\frac{\{J(J\;+\;1)\}^{1/2}}{2J\;+\;1}\frac{1}{(pq)^{J-1}}\left[B_{J-1}^{(\pm)} \;-\; B_{J+1}^{(\pm)}\right]. \qquad (14)$$

The lower index describes the helicity of the $N\bar{N}$ state; $\pm$ corresponds to $\lambda_N=\pm\frac{1}{2}$, $\lambda_{\bar{N}}=+\frac{1}{2}$. The Pauli principle puts constraints on these amplitudes: $f_\pm^{J\,(-)}=0$ for even J and $f_\pm^{J\,(+)}=0$ for odd J; therefore, the isospin index ($\pm$) is usually omitted.

At this point it is necessary to specify the set of operators $\hat{C}_j$ which we will use in order to represent the $NN \to NN$ as well as the $N\bar{N} \to N\bar{N}$ amplitude, i.e., T_s and T_t. There are two possible operators in isospin space, $I_2^{(1)}I_2^{(2)}$ (I_n is the $n\times n$ identity matrix) and $\boldsymbol{\tau}^{(1)}\cdot\boldsymbol{\tau}^{(2)}$. We can therefore define

$$\hat{C}_j \;=\; 3I_2^{(1)}I_2^{(2)}\hat{C}_j^{(+)},$$
$$\hat{C}_{j+5} \;=\; 2\boldsymbol{\tau}^{(1)}\cdot\boldsymbol{\tau}^{(2)}\hat{C}_j^{(-)}, \qquad (15)$$

for $j=1,...,5$. $\hat{C}_j^{(\pm)}$ act only in the two-nucleon spin space. Here, we use

$$\hat{C}_1^{(+)} = I_4^{(1)} I_4^{(2)}, \ \hat{C}_2^{(+)} = -(\gamma^{(1)} \cdot N_2 I_4^{(2)} + I_4^{(1)} \gamma^{(2)} \cdot N_1),$$
$$\hat{C}_3^{(+)} = \gamma^{(1)} \cdot N_2 \gamma^{(2)} \cdot N_1, \ \hat{C}_4^{(+)} = \gamma^{(1)} \cdot \gamma^{(2)}, \ \hat{C}_5^{(+)} = \gamma_5^{(1)} \gamma_5^{(2)} \quad (16)$$

with $N_i \equiv \frac{1}{2}(p_i + p_i')$ and

$$\hat{C}_1^{(-)} = N_1 \cdot N_2 I_4^{(1)} I_4^{(2)}, \ \hat{C}_j^{(-)} = \hat{C}_j^{(+)}, \ j = 2, ..., 5 . \quad (17)$$

The slightly different set for $\hat{C}_j^{(-)}$ is used in order to have from the beginning the operator structure of ρ exchange, given by $\hat{C}_{1,2,4}^{(-)}$.

In a lengthy but straightforward calculation (cf. Ref. [16]) one now expands both sides of the unitarity relation [Eq. (8)] in terms of $C_j(t)$ (defined as matrix elements of $\hat{C}_j$ sandwiched between the appropriate Dirac spinors and Pauli isospinors for the t channel [Eq. (6)]), using the fact that

$$A_{\alpha\beta} = \delta_{\alpha\beta} A^{(+)} + \frac{1}{2} [\tau_\beta, \tau_\alpha] A^{(-)} \quad (18)$$

and the same for B. A comparison of coefficients leads to

$$\mathrm{Im} c_1^{J=0}(t') = -8\pi \left(\frac{t' - 4m_\pi^2}{t'} \right)^{1/2} \frac{1}{(t' - 4m_N^2)^2} \mid f_+^{J=0}(t') \mid^2 \quad (19)$$

for the scalar contribution, and

$$\mathrm{Im} c_6^{J=1}(t') = -6\pi \frac{(t' - 4m_\pi^2)^{3/2}}{t'^{1/2} (t' - 4m_N^2)^2} \left[\left| f_+^{J=1}(t') \right|^2 + \frac{m_N^2}{2} \left| f_-^{J=1}(t') \right|^2 - \sqrt{2} m_N \mathrm{Re} \left\{ f_-^{J=1\,*}(t') f_+^{J=1}(t') \right\} \right],$$
$$\mathrm{Im} c_7^{J=1}(t') = -\frac{3}{2}\pi \frac{(t' - 4m_\pi^2)^{3/2}}{t'^{1/2} (t' - 4m_N^2)} \left[\frac{m_N}{2} \left| f_-^{J=1}(t') \right|^2 - \frac{1}{\sqrt{2}} \mathrm{Re} \left\{ f_-^{J=1\,*}(t') f_+^{J=1}(t') \right\} \right],$$
$$\mathrm{Im} c_9^{J=1}(t') = \frac{3}{16}\pi \frac{(t' - 4m_\pi^2)^{3/2}}{t'^{1/2}} \mid f_-^{J=1}(t') \mid^2 \quad (20)$$

for the vector contribution. The other coefficients are zero.

C. Microscopic model for the $N\bar{N} \to 2\pi$ process

In the last section we have outlined the way which leads from the $N\bar{N} \to 2\pi$ partial wave helicity amplitudes $f_\pm^J$ [Eq. (14)] to the 2π-exchange contribution to the $NN \to NN$ scattering amplitude. Usually, in dispersion theoretical derivations of the NN interaction (cf. Refs. [5–8]), the $f_\pm^J$ are taken from "quasiempirical" information obtained by analytic continuation of πN as well as $\pi\pi$ scattering data [14]. As we have discussed in the Introduction, it is essential for our purposes to follow an alternative procedure, since a consistent treatment of medium modifications requires the construction of a truly dynamical model for the $N\bar{N} \to 2\pi$ amplitude, not only for the elementary $N\bar{N} \to 2\pi$ transition but also for the $\pi\pi \to \pi\pi$ amplitude.

The ingredient of our model is visualized in Fig. 6: It consists of an $N\bar{N} \to 2\pi$ transition, $V_{N\bar{N}\to 2\pi}$, with nucleon as well as Δ exchange. $V_{N\bar{N}\to 2\pi}$ is essentially taken from the former work of the Jülich group dealing with the $N\bar{N}$ system [18,19], which started from the following Lagrangians:

$$\mathcal{L}_{\pi NN} = \frac{f_{\pi NN}}{m_\pi} \bar{\psi}(x) \gamma^5 \gamma^\mu \boldsymbol{\tau} \psi(x) \cdot \partial_\mu \boldsymbol{\phi}_\pi(x), \quad (21)$$

$$\mathcal{L}_{\pi N\Delta} = \frac{f_{\pi N\Delta}}{m_\pi} \bar{\Psi}^\mu(x) \mathbf{T} \psi(x) \cdot \partial_\mu \boldsymbol{\phi}_\pi(x) + \mathrm{H.c.} \quad (22)$$

The only difference is that we now take into account nonpole contributions to the Δ propagator according to the Rarita-Schwinger choice:

$$G_{\mu\nu}^{(\pm)}(k) = \frac{1}{\not{k} - m_\Delta} \left[-g_{\mu\nu} + \frac{1}{3}\gamma_\mu\gamma_\nu + \frac{2}{3m_\Delta^2} k^\mu k^\nu - \frac{1}{3m_\Delta} (k_\mu \gamma_\nu - \gamma_\mu k^\nu) \right] + \frac{1}{3m_\Delta^2} [\gamma_\mu (\not{k} - m_\Delta) \gamma_\nu - (\gamma_\mu k_\nu + k_\mu \gamma_\nu)] \quad (23)$$

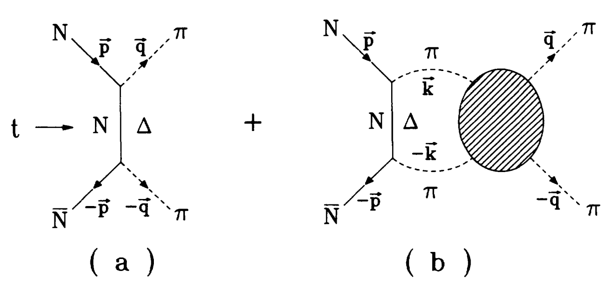

FIG. 6. Our dynamical model for the $N\bar{N} \to 2\pi$ amplitude. The $\pi\pi \to \pi\pi$ amplitude in (b) is taken from Lohse *et al.* [12].

with $k \equiv p - q$. As usual, phenomenological form factors $F_{N,\Delta}$ have been added to account for the extended vertex structure. They are parametrized by

$$F_{N,\Delta} = \left(\frac{n\Lambda_{N,\Delta}^2 - m_{N,\Delta}^2}{n\Lambda_{N,\Delta}^2 + (\mathbf{p}-\mathbf{q})^2} \right)^n \tag{24}$$

with cutoff masses to be determined later.

The full $N\bar{N} \to 2\pi$ amplitude is obtained from

$$T_{N\bar{N}\to 2\pi} = V_{N\bar{N}\to 2\pi} + T_{2\pi\to 2\pi} G_{2\pi} V_{N\bar{N}\to 2\pi} \tag{25}$$

with $T_{2\pi\to 2\pi}$ taken from Ref. [12], or, more explicitly,

$$\langle \mathbf{q}00|T(E_z)|\mathbf{p}\lambda_N\lambda_{\bar{N}}\rangle = \langle \mathbf{q}00|V|\mathbf{p}\lambda_N\lambda_{\bar{N}}\rangle + \int d^3k \langle \mathbf{q}00|T(E_z)|\mathbf{k}00\rangle \frac{1}{E_z - 2\omega_k + i\epsilon} \langle \mathbf{k}00|V|\mathbf{p}\lambda_N\lambda_{\bar{N}}\rangle \tag{26}$$

with the starting energy $E_z = 2E_p = \sqrt{t'}$. Note that both T amplitudes in Eq. (26) are related to the S matrix by

$$S_{fi} = \delta_{fi} - i(2\pi)\delta^{(4)}(P_f - P_i)T_{fi}. \tag{27}$$

We define partial wave amplitudes according to

$$\langle 00|V^J(q,p)|\lambda_N\lambda_{\bar{N}}\rangle = 2\pi \int_{-1}^{1} d(\cos\theta) d_{\lambda 0}^J(\cos\theta) \langle \mathbf{q}00|V|\mathbf{p}\lambda_N\lambda_{\bar{N}}\rangle, \tag{28}$$

where $d_{\lambda 0}^J$ are the conventional reduced rotation matrices, and $\lambda \equiv \lambda_N - \lambda_{\bar{N}}$. We then obtain the partial wave expansion

$$\langle \mathbf{q}00|V|\mathbf{p}\lambda_N\lambda_{\bar{N}}\rangle = \frac{1}{4\pi} \sum_J (2J+1) d_{\lambda 0}^J(\cos\theta) \langle 00|V^J(q,p)|\lambda_N\lambda_{\bar{N}}\rangle \tag{29}$$

and similarly for T, which leads to the partial wave decomposition of Eq. (26),

$$\langle 00|T^J(q,p;E_z)|\lambda_N\lambda_{\bar{N}}\rangle = \langle 00|V^J(q,p)|\lambda_N\lambda_{\bar{N}}\rangle + \int_0^\infty dk k^2 \langle 00|T^J(q,k)|00\rangle \frac{1}{E_z - 2\omega_k + i\epsilon} \langle 00|V^J(k,p)|\lambda_N\lambda_{\bar{N}}\rangle. \tag{30}$$

This equation can be solved numerically. The on-shell amplitudes are related to the required helicity amplitudes $f_\pm^J$ in the following way:

$$f_+^J(t') = -\pi \frac{1}{4} E_z^2 p \frac{1}{(pq)^J} \left\langle 00 \middle| T^J(q,p;E_z) \middle| \frac{1}{2}\frac{1}{2} \right\rangle,$$
$$f_-^J(t') = -\pi \frac{1}{2} E_z p \frac{1}{(pq)^J} \left\langle 00 \middle| T^J(q,p;E_z) \middle| \frac{1}{2} - \frac{1}{2} \right\rangle. \tag{31}$$

Note that in the pseudophysical region $(4m_\pi^2 \le t' \le 4m_N^2)$ p is imaginary.

D. NN interaction arising from correlated 2π exchange

If we insert the resulting $f_\pm^J$ into Eqs. (19) and (20) we then obtain, by means of Eq. (7), the 2π-exchange contribution to the NN interaction. However, by construction (see Fig. 6), this result contains not only the correlated part we are interested in but also the uncorrelated contribution, cf. Fig. 1. Therefore, the latter part has to be removed. We do this by identifying $f_{\pm,B}^J$ as the corresponding amplitudes for the Born terms [Fig. 6(a)] and putting, in complete analogy to Eqs. (19) and (20),

$$\mathrm{Im}c_{1,B}^{J=0}(t') = -8\pi \left(\frac{t'-4m_\pi^2}{t'}\right)^{1/2} \frac{1}{(t'-4m_N^2)^2} \mid f_{+,B}^{J=0}(t') \mid^2,$$
$$\mathrm{Im}c_{6,B}^{J=1}(t') = -6\pi \frac{(t'-4m_\pi^2)^{3/2}}{t'^{1/2}(t'-4m_N^2)^2} \left[\left|f_{+,B}^{J=1}(t')\right|^2 + \frac{m_N^2}{2} \left|f_{-,B}^{J=1}(t')\right|^2 - \sqrt{2} m_N \mathrm{Re}\left\{ f_{-,B}^{J=1\,*}(t') f_{+,B}^{J=1}(t') \right\} \right],$$
$$\mathrm{Im}c_{7,B}^{J=1}(t') = -\frac{3}{2}\pi \frac{(t'-4m_\pi^2)^{3/2}}{t'^{1/2}(t'-4m_N^2)} \left[\frac{m_N}{2} \left|f_{-,B}^{J=1}(t')\right|^2 - \frac{1}{\sqrt{2}} \mathrm{Re}\left\{ f_{-,B}^{J=1\,*}(t') f_{+,B}^{J=1}(t') \right\} \right],$$
$$\mathrm{Im}c_{9,B}^{J=1}(t') = \frac{3}{16}\pi \frac{(t'-4m_\pi^2)^{3/2}}{t'^{1/2}} \mid f_{-,B}^{J=1}(t') \mid^2 . \tag{32}$$

The NN interaction due to correlated 2π exchange may then be written as

$$V_{2\pi,\mathrm{corr}} = V^{(S)}_{2\pi,\mathrm{corr}} + V^{(P)}_{2\pi,\mathrm{corr}} = \frac{\kappa}{\pi}\int_{4m_\pi^2}^{\infty}\frac{\rho_1^{(+)}(t')}{t'-t}dt' C_1^{(+)} + \frac{\kappa}{\pi}\sum_{j=1,2,4}\int_{4m_\pi^2}^{\infty}\frac{\rho_j^{(-)}(t')}{t'-t}dt' C_j^{(-)}\boldsymbol{\tau}_1\cdot\boldsymbol{\tau}_2 \tag{33}$$

with the spectral functions $\rho_j^{\pm}$ given by

$$\rho_1^{(+)}(t') = 3\left[\mathrm{Im}c_1^{J=0}(t') - \mathrm{Im}c_{1,B}^{J=0}(t')\right],$$
$$\rho_j^{(-)}(t') = 2\left[\mathrm{Im}c_{j+5}^{J=1}(t') - a\mathrm{Im}c_{j+5,B}^{J=1}(t')\right],\ j=1,2,4. \tag{34}$$

The factor $\kappa = \frac{1}{(2\pi)^3}\frac{m_N^2}{\sqrt{E_1E_1'E_2E_2'}}$ arises since $V_{2\pi,\mathrm{corr}}$ is to be defined as part of the Bonn potential whose T matrix fulfills Eq. (27). The $C_j^{(\pm)}$ are specific matrix elements between Dirac spinors in the helicity representation, in the s channel. Furthermore, if $\mathbf{p}(\mathbf{p}')$ denotes the initial (final) c.m. three-momentum of the NN system, the momentum transfer variable t can be written as $t = -(\mathbf{p}'-\mathbf{p})^2$ (with the on-shell condition $\mathbf{p}'^2 = \mathbf{p}^2$) and $s = 4E_p^2$. Therefore, the result Eq. (33) can be represented as in the Bonn potential, i.e., as an (on-shell) matrix element $\langle \mathbf{p}'\lambda_1'\lambda_2'|V_{2\pi,\mathrm{corr}}|\mathbf{p}\lambda_1\lambda_2\rangle$. The partial wave decomposition can then be defined in precisely the same way as in Ref. [10] using a generalization of Eq. (29).

III. RESULTS AND DISCUSSION

A. $N\bar{N}\to 2\pi$ amplitudes $f_\pm^J$

In order to evaluate the $N\bar{N}\to 2\pi$ amplitudes it remains to specify the parameters in the $N\bar{N}\to 2\pi$ transition potential. The relevant masses used are $m_N = 938.926$ MeV, $m_\Delta = 1232$ MeV, and $m_\pi = 138.03$ MeV. For the coupling constants (unless stated otherwise), the same values are used as in the Bonn potential, i.e., $f^2_{NN\pi}/4\pi = 0.0778$ and $f^2_{N\Delta\pi}/4\pi = 0.224$. On the other hand, form factor parameters should not be blindly taken over from the Bonn potential. The reason is that for the t-channel baryon exchange process considered here one is in a quite different kinematic regime from that of the physical s-channel pion-exchange process. The fact that we cannot establish a definite relation for the πNN vertex in different kinematic domains is the price we have to pay for our simplified treatment of the πNN vertex structure, which makes the form factor depend on the momentum of only one particle [cf. Eq. (24)]. This is a general problem which, in our opinion, is difficult to avoid, since a reliable QCD calculation of the full momentum dependence of the vertex does not exist.

Fortunately, as mentioned before, there is quasiempirical information about the $f_\pm^J$ in the pseudophysical region obtained by analytic continuation of empirical πN and $\pi\pi$ data [14]. We use this information to constrain cutoff masses $\Lambda_N, \Lambda_\Delta$ in the form factor, Eq. (24), to the values $\Lambda_N(\Lambda_\Delta) = 1.9$ (2.1) GeV. Note that the parametrization in the form factor is chosen such that the dependence on n is quite weak; we take n_N (n_Δ) to be 1 (2).

There is one amplitude, f_+^0, for the scalar (σ) channel whereas there are two, f_+^1 and f_-^1, for the vector (ρ) channel. In Fig. 7 we show the results in the pseudophysical region obtained from our dynamical model, for both the real and imaginary parts. Obviously the nucleon exchange dominates; however, the Δ contribution is non-negligible, especially in the f_1^- amplitude.

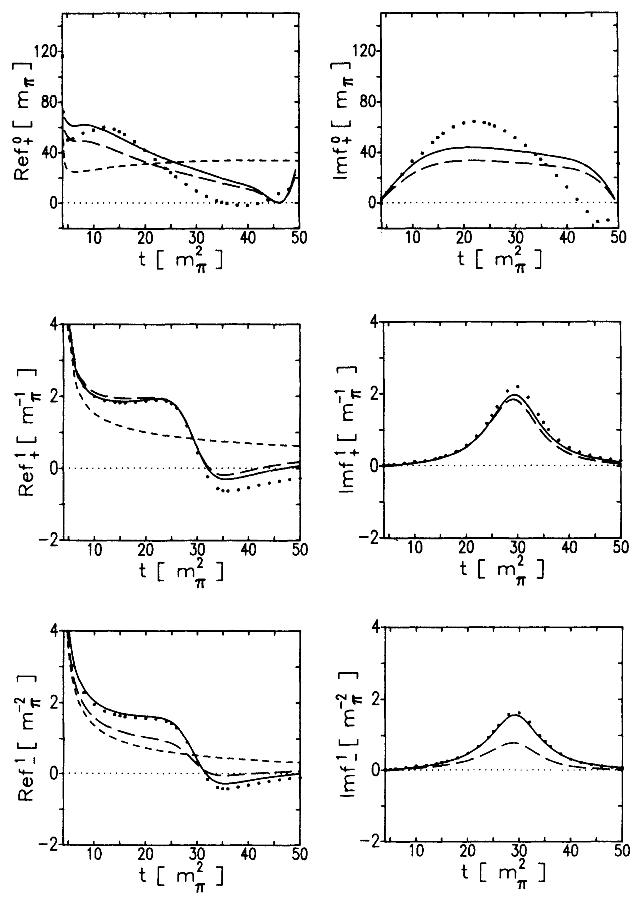

FIG. 7. The $N\bar{N}\to 2\pi$ helicity amplitudes $f_\pm^{0,1}(t)$ defined in the text and as function of t in the pseudophysical region, as predicted by our dynamical model. The solid line denotes the total result while the long-dashed line gives the contribution provided by N exchange only. The short-dashed line is provided by the $(N+\Delta)$ Born terms. The curve indicated by dots shows the quasiempirical result obtained by analytic continuation of πN and $\pi\pi$ data, taken from Ref. [14].

Given that we have only two open parameters $(\Lambda_N, \Lambda_\Delta)$ there is remarkable agreement with the quasiempirical result [14] in all vector amplitudes. Some disagreement occurs in the scalar channel. Fortunately, as we will discuss, these do not severely affect our final result: the correlated 2π-exchange potential. Furthermore one should keep in mind that the quasiempirical result is subject to considerable uncertainty at large values of t'.

B. The spectral functions $\rho_j^{(\pm)}$

Next, we show in Fig. 8 the spectral functions defined in Eq. (34), namely $\rho_1^{(+)}$ for the scalar channel and $\rho_j^{(-)}$ $(j = 1, 2, 4)$ for the vector channel. Note that for both the dynamical model and the quasiempirical result we have subtracted precisely the same (N and Δ exchange) Born terms as given by our dynamical model in order to allow for a meaningful comparison. As expected from the foregoing section, there is good agreement with the quasiempirical result in the vector channel but discrepancies occur in the scalar channel. As indicated in the figure, the use of σ' and ρ exchange with sharp masses $m_{\sigma'} = 550$ MeV, $m_\rho = 769$ MeV, as done in the Bonn potential, corresponds to a delta-function behavior at the corresponding t' value.

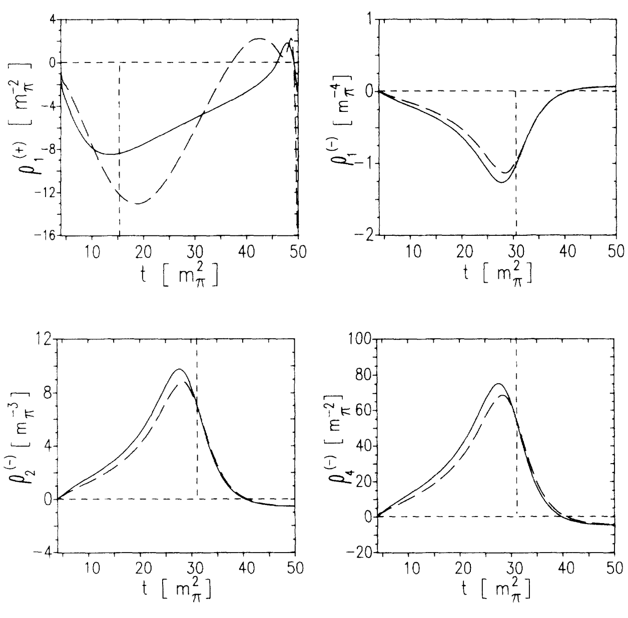

FIG. 8. Spectral functions $\rho_1^{+}(t')$ $(\rho_i^{(-)}, i = 1, 2, 4)$ as defined in the text and as function of t' in the pseudophysical region, characterizing the correlated 2π-exchange contribution to the NN interaction in the scalar-isoscalar (vector-isovector) channel. The solid line shows the prediction of our dynamical model whereas the dashed line shows the result obtained from the quasiempirical information [14]. The vertical lines indicate the δ function at $m_{\sigma'} = 550$ MeV ($m_\rho = 769$ MeV), representing sharp mass σ' and ρ exchange as used in the Bonn potential.

C. (On-shell) potentials for correlated 2π exchange

From the spectral functions $\rho_j^{(\pm)}$ the NN interaction arising from correlated 2π exchange, $V_{2\pi,\text{corr}}$, can then be obtained by means of Eq. (33). For our practical calculations we use a cutoff $t_c = 50m_\pi^2$ in the dispersion integral. Such a cutoff procedure is customary in dispersion theoretical treatments and is done mainly because both our dynamical model and the quasiempirical result cannot be trusted for considerably larger t'. For the small momentum transfers t of interest here, the weighting factor t'^{-1} in the dispersion integral strongly suppresses the sensitivity to variations of t_c. As described briefly at the end of Sec. II C, LSJ partial wave states of $V_{2\pi,\text{corr}}$ can be obtained in a straightforward way.

1. σ channel

We first discuss the results in the scalar channel. Figure 9 shows the (on-shell) potentials $V_{2\pi,\text{corr}}$ as a func-

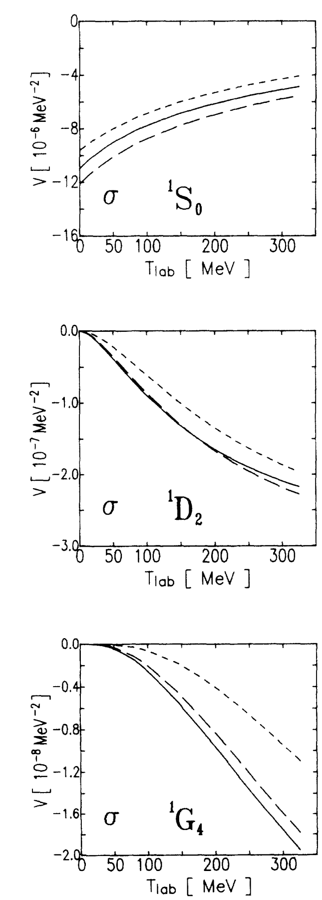

FIG. 9. On-shell potentials in various NN partial waves arising from correlated 2π exchange in the scalar channel, as function of the nucleon laboratory kinetic energy. The solid lines are predictions of our dynamical model whereas the long-dashed lines are derived from the quasiempirical result of Ref. [14]. The short-dashed lines denote the contribution of (sharp mass) σ' exchange as used in the Bonn potential [10], including the form factor.

tion of $T_{\rm lab}$ in the NN spin singlet states with (relative) angular momentum $L = 0, 2, 4$, i.e., using the common notation $^{2S+1}L_J$, in the $^1S_0$, $^1D_2$, and $^1G_4$ state. As expected, our dynamical model provides attraction in all partial waves. There is remarkable overall agreement between the model predictions and the quasiempirical results despite sizable differences in the spectral function $\rho_1^{(+)}$. This is easily understood since what counts in a first approximation is just the area under the spectral function, which is quite similar for both cases. A closer look however shows that our model is practically identical to the quasiempirical result in $^1D_2$ but somewhat smaller (larger) in $^1S_0$ ($^1G_4$), which means that our model prediction has a slightly longer range. Obviously, the lower t' portion of the spectral function (where our model is larger than the quasiempirical result) has, indeed, a strong weight for the determination of the 2π-exchange potential, a fact which confirms the justification of the cutoff procedure discussed before.

Compared to both the model and quasiempirical result, the (sharp mass) σ' contribution used in the Bonn potential differs remarkably in higher partial waves, whereas it is similar in the $^1S_0$ state. Note that the σ' contribution contains the phenomenological vertex form factor of monopole type with a cutoff mass of 2 GeV as used in the Bonn potential. The strong underestimation (by about a factor of 2) in $^1G_4$ is due to the missing of the long-range (small t') tail in the spectral function. Obviously, and not unexpectedly, a broad mass distribution cannot be replaced by a sharp mass if a truly quantitative description over all relevant partial waves is to be kept. The procedure done in Ref. [10], namely to replace a broad σ' exchange with $g^2_{\sigma'}/4\pi = 10$, $m_{\sigma'} = 662.5$ MeV and $\Gamma_{\sigma'} = 524.5$ MeV (considered in the first place) by the sharp σ' exchange (cf. Sec. 5 of Ref. [10]) is necessarily quite rough. In fact, Fig. 7 of Ref. [10] shows clearly that (at medium energies) the replacement works well for F waves but underestimates the broad distribution in higher partial waves, e.g., $^3H_6$. Conversely, in lower partial waves (not shown in [10]) the sharp σ' provides a stronger contribution.

If we go back to our results and look at the systematics of Fig. 9, we expect that in an F wave the sharp σ' would be about 2/3 of the dispersion theoretical result (which we have confirmed by an actual calculation). Taking into account the foregoing discussion, this then implies that the present result for correlated 2π exchange is larger by about 30% than the broad σ' discussed in Ref. [10]. This is indeed true: The dispersion theoretical calculation of Ref. [11], which practically agrees with the quasiempirical information [14], yields for the 2π-exchange contribution, according to Ref. [11], $g^2_{\sigma'}/4\pi = 13$ instead of 10 used in Ref. [10], with all other parameters being the same. Furthermore, the subtraction of N, Δ Born terms in Ref. [11] is larger since there a larger $N\Delta\pi$ coupling constant was used ($f^2_{N\Delta\pi}/4\pi = 0.36$ instead of 0.224 used here). Consequently, with our $N\Delta\pi$ coupling constant, the resulting $g^2_{\sigma'}/4\pi$ should be around 15 or so, indeed about 50% larger than the σ' used in Ref. [10].

Thus, the different property of the sharp σ' used in Ref. [10] compared to a realistic evaluation of correlated 2π exchange arises from two facts. First, the overall strength of the σ' is about 30% too small; second, the sharp mass approximation leads to an additional underestimation of high ($L \geq 4$) partial waves but an overestimation in low partial waves, which roughly cancels the former underestimation. Combining both effects the sharp σ' obviously provides a reasonable description of the situation in S and P waves but strongly underestimates the contribution in high partial waves, see Fig. 9.

2. ρ channel

We now turn our attention to the vector channel. Figure 10 shows again the on-shell potentials $V_{2\pi,\rm corr}$ in the $^1S_0$, $^1P_1$ state and $^3SD_1$ transition. Again, our dynamical model prediction and the quasiempirical result are in qualitative agreement. In contrast to the scalar channel, this fact was to be anticipated since both spectral functions agree quite well.

Compared to the single ρ exchange used in the Bonn

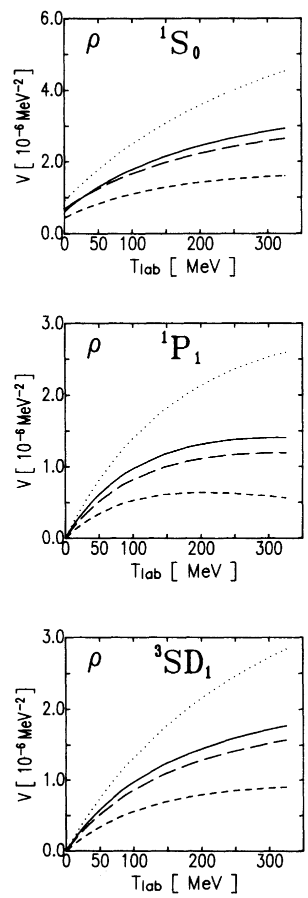

FIG. 10. On-shell potentials in various NN partial waves arising from correlated 2π exchange in the vector channel as function of the nucleon laboratory kinetic energy. The solid lines are predictions of our dynamical model whereas the long-dashed lines are derived from the quasiempirical result of Ref. [14]. The short-dashed (dotted) lines denote the contribution of sharp mass ρ exchange as used in the Bonn potential [10], with (without) the form factor.

potential, the realistic evaluation of correlated 2π exchange provides a much larger result (by a factor of 2 or so) in all partial waves. One reason is that, in the Bonn potential, a phenomenological (monopole) form factor is added to the $NN\rho$ vertex, with a cutoff mass of $\Lambda_\rho = 1.4$ GeV for both vector and tensor coupling. This form factor, while being correctly normalized to 1 at the meson pole, becomes less than 0.5 at $t=0$, which implies that both the strength of vector and tensor coupling (for the definition, see Ref. [10]) are reduced by more than 50% in the physical region.

The problem is that such a strong suppression from the pole into the physical region is not provided by the realistic calculation, as can be seen by defining effective couplings $F_i(t)$. Motivated by the OBE expression for sharp ρ exchange (without form factors)

$$\bar{V}_\rho = \frac{f_{\rho NN}^2}{m_N^2}\frac{1}{m_\rho^2-t}C_1^{(-)} + \frac{f_{\rho NN}g_{\rho NN}}{m_N}\left(1+\frac{f_{\rho NN}}{g_{\rho NN}}\right)\frac{1}{m_\rho^2-t}C_2^{(-)} + g_{\rho NN}^2\left(1+\frac{f_{\rho NN}}{g_{\rho NN}}\right)^2 C_4^{(-)}, \tag{35}$$

we parametrize our result as

$$V_{2\pi,\mathrm{corr}}^{(P)} = \frac{F_1(t)}{m_N^2}\frac{1}{m_\rho^2-t}C_1^{(-)} + \frac{F_2(t)}{m_N}\frac{1}{m_\rho^2-t}C_2^{(-)} + F_4(t)\frac{1}{m_\rho^2-t}C_4^{(-)}, \tag{36}$$

which leads to

$$F_1(t) = \frac{m_N^2}{\pi}(m_\rho^2-t)\int_{4m_\pi^2}^{t_c}\frac{\rho_1^{(-)}(t')}{t'-t}dt',$$

$$F_2(t) = \frac{m_N}{\pi}(m_\rho^2-t)\int_{4m_\pi^2}^{t_c}\frac{\rho_2^{(-)}(t')}{t'-t}dt',$$

$$F_4(t) = \frac{1}{\pi}(m_\rho^2-t)\int_{4m_\pi^2}^{t_c}\frac{\rho_4^{(-)}(t')}{t'-t}dt'. \tag{37}$$

Figure 11 compares the tensor coupling strength, i.e., $\frac{f_{\rho NN}^2}{4\pi}\cdot F_\rho^2(t)$, $F_\rho = \frac{\Lambda_\rho^2-m_\rho^2}{\Lambda_\rho^2-t}$ with $\Lambda_\rho = 1.4$ GeV, as used in the Bonn potential, with $\frac{F_1(t)}{4\pi}$ as obtained in our dynamical model calculation. The same is done for the vector coupling, $\frac{g_{\rho NN}^2}{4\pi}\cdot F_\rho^2(t)$ versus $\frac{1}{4\pi}[F_4(t)-2F_2(t)-F_1(t)]$, and for $f_{\rho NN}/g_{\rho NN}$ versus $F_1(t)/[F_2(t)-F_1(t)]$. We make the following observations.

(1) The dispersion theoretical result has quite a weak t dependence reducing the values by about 20% only over the t range considered in agreement with the result obtained by Höhler and Pietarinen [20] which is based on essentially the same $N\bar{N}\to 2\pi$ input; on the other hand, the rather soft form factor in the Bonn potential reduces it by more than 50%.

(2) At $t=0$, our present result for the dominant tensor coupling [Fig. 11(a)] is about twice as large as the value used in the Bonn model; this explains Fig. 10.

(3) Concerning the vector coupling [Fig. 11(b)], there is also an increase at $t=0$ by about 60%. Consequently, the effective tensor to vector ratio increases from 6.1 as used in the Bonn model to a value of about 7.

D. NN scattering phase shifts

"Theoretical" NN scattering phase shifts are obtained from the on-shell scattering amplitude, which is usually found as a solution of a scattering equation of Lippmann-Schwinger type, with some interaction V_{NN} as input [cf. Eq. (25) for the $N\bar{N}\to 2\pi$ amplitude]. In order to obtain such a solution, V_{NN} has to be known (half) off shell. However dispersion theory is an on-shell theory, i.e., it can only provide information about on-shell pieces of the amplitude; therefore, in order to apply $V_{2\pi,\mathrm{corr}}$ in a scattering equation, it has to be extrapolated off shell in

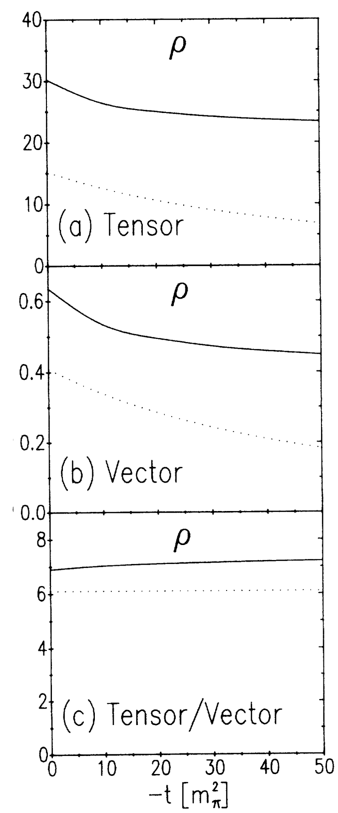

FIG. 11. The effective vector coupling constants $f_\rho^2(t)/4\pi$, $g_\rho^2(t)/4\pi$, and the ratio $f_\rho/g_\rho(t)$ predicted by our dynamical model in the physical region of NN scattering ($t\le 0$), as defined in the text and based on $m_\rho = 769$ MeV (solid line). The corresponding values used in the Bonn potential including the form factor are indicated by the dotted lines.

some way. This is a weak point in dispersion theoretical derivations of potentials, and the price we have to pay for concentrating in our derivation on the t channel. Indeed, as discussed in the Introduction, we could have directly evaluated $V_{2\pi,\mathrm{corr}}$ in the s channel and, given our field theoretical $\pi\pi \to \pi\pi$ amplitude, would have obtained a well-defined off-shell behavior for $V_{2\pi,\mathrm{corr}}$. It should be pointed out however that such a calculation is more complicated, since two-loop integrals are involved in this case. Furthermore, given that our $\pi\pi$ T matrix is not crossing symmetric, we cannot be sure that the result will be reliable in the t channel, which determines the main dynamics of the interaction. Finally, since $V_{2\pi,\mathrm{corr}}$ is already a second-order contribution, off-shell effects (which arise at the outer legs) enter only in still higher order of T_{NN} and are therefore of comparably reduced importance.

Nevertheless, we will avoid the problem of extrapolating $V_{2\pi,\mathrm{corr}}$ off shell in this paper, by restricting ourselves to phase shifts in high angular momentum partial waves. For these, the Born approximation is an extremely good approximation, which means here taking only the lowest order term in the R-matrix equation

$$R(E) = V + V \frac{\mathcal{P}}{E - H_0} R(E) \tag{38}$$

with R being related to the conventional T matrix by

$$T(E) = R(E) - i\pi R(E)\delta(E - H_0)T(E) \tag{39}$$

and $\mathcal{P}$ denotes the principal value. Note that the Born approximation defined in this way, often called K-matrix approximation, is unitary. Needless to say that putting $R(E) = V$ requires the knowledge of V only on shell.

In order to have a meaningful comparison both with experiment and sharp σ', ρ exchange used in the Bonn potential, we will supplement $V_{2\pi,\mathrm{corr}}$ (i) by single π and ω exchange, and (ii) by the uncorrelated 2π-exchange contribution of Fig. 1. (Note that the second iteration of the one-pion exchange is included in the latter contribution.) The parameters are taken to be precisely the same as in Sec. 5 of Ref. [10], i.e., $f^2_{NN\pi}/4\pi = 0.0778$ ($\simeq g^2_{NN\pi}/4\pi = 14.4$), $f^2_{N\Delta\pi}/4\pi = 0.224$, $m_\pi = 138.03$ MeV, $g^2_{NN\omega}/4\pi = 5.7$, $m_\omega = 783$ MeV. Monopole form factors with cutoff masses $\Lambda_{NN\pi} = 1.3$ GeV, $\Lambda_{N\Delta\pi} = 1.2$ GeV have been used for the evaluation of the diagrams in Fig. 1. Since the high angular momentum phase shifts to be considered depend only on the long-range part of the amplitude, they are almost independent of form factor parameters.

At this point it is perhaps worthwhile to point out that the above values for the coupling constants ($f^2_{NN\pi}$, $f^2_{N\Delta\pi}$) agree with those used in our dynamical model for the $N\bar{N} \to 2\pi$ amplitude. This is—of course—done on purpose, since it is an essential requirement for consistency. In order to isolate the correlated 2π exchange, we have subtracted from the total $N\bar{N} \to 2\pi$ amplitude (which is constrained by quasiempirical information) the elementary ($N + \Delta$ exchange) transition. Thus, our procedure amounts to first subtracting the uncorrelated contributions in the t channel and then adding them back in the s channel. The importance of using the same parameters is obvious.

Due to our oversimplified treatment of form factors this can however not be done for the cutoff mass since we cannot be sure that this parameter is the same in both the t channel (where it parametrizes the off-shell behavior of N, Δ) as well as in the s channel (where it describes the corresponding behavior of the pion). Thus the cutoff mass in the s channel remains an open parameter. Fortunately, this ambiguity does not affect our conclusions in this paper since, as mentioned before, high partial waves only slightly depend on form factors. We would like to point out already here that the low partial waves, which are affected by this ambiguity, are—in any case—subject to uncertainties generated by the choice of off-shell extension of $V_{2\pi,\mathrm{corr}}$. In this connection we mention also that the different choice of the Δ propagator in our model for $N\bar{N} \to 2\pi$ (taking into account nonpole contributions) compared to the Bonn potential where these are left out affects the consistency only in a negligible way since in the s channel, the Δ is not far off shell, and the pole contribution by far dominates.

The question might arise why we subtract and then add the uncorrelated 2π exchange anyhow. Why not transform the total 2π-exchange amplitude (without any subtraction) into the s channel and then leave out the uncorrelated contributions of Fig. 1? There are several arguments for not choosing this alternative. First, such a procedure includes only the $J^P = 0^+, 1^-$contributions (in the t channel) of Fig. 1 whereas our treatment is more complete since the diagrams of Fig. 1 (evaluated directly in the s channel) contain automatically all higher $J \geq 2$ t-channel contributions. On the other hand, our restriction to $J = 0^+, 1^-$ contributions of the correlated part is probably justified since in this case the higher J^P pieces are known to be small; e.g., the $f(2^+)$ resonance occurs at about 1250 MeV— too large to be important for low energy NN scattering. Note also that, for a calculation of low partial wave phase shifts, the iterative box diagrams involving NN intermediate states have to be subtracted in any case since they are unavoidably generated by the scattering equation.

Second, since our ultimate goal is to derive a coupled-channel model, i.e., to treat the N and Δ on an equal footing, we must keep the diagrams of Fig. 1 explicitly. We mention that Haidenbauer, Holinde, and Johnson [21] recently presented such a coupled-channel model based essentially on the physics of the Bonn potential and the method of folded diagrams.

Finally, for the purpose of the present paper, which is to compare the role of a realistic treatment of correlated 2π exchange versus (sharp) σ', ρ exchange used in the Bonn potential, it is necessary to treat the other contributions (single π, ω exchange, uncorrelated 2π exchange) precisely the same as in Ref. [10].

Figure 12 presents the results for some selected high angular momentum partial wave np phase shifts (obtained in Born approximation as defined and as function of the lab kinetic energy)—namely those for which empirical information is available. Here, we wish to demonstrate the role of the various models for correlated 2π exchange: (i) our dynamical model, (ii) the model derived

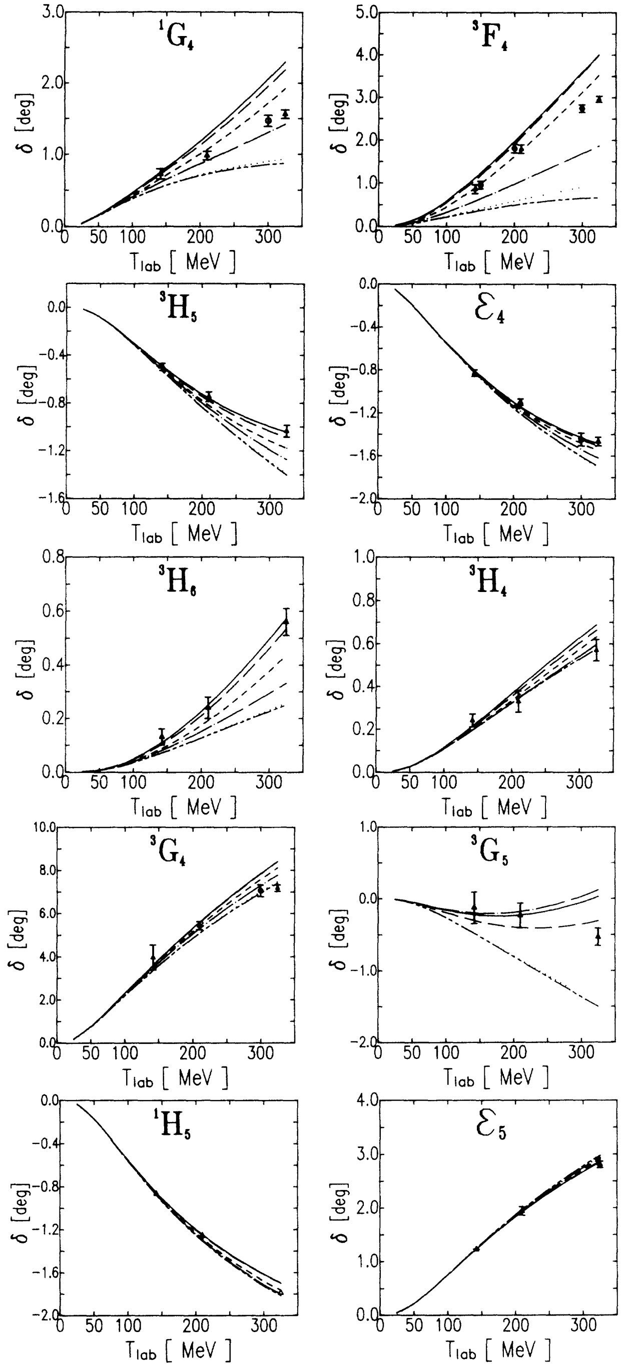

FIG. 12. *np* phase shifts as function of the nucleon laboratory kinetic energy, predicted by our dynamical model for correlated 2π exchange (solid line), supplemented by π exchange and ω exchange ($g^2_{NN\omega}/4\pi = 5.7$) and the uncorrelated 2π-exchange contributions as calculated in the Bonn potential [10], using $g^2_{NN\pi}/4\pi = 14.4$. In the long-dashed line, the correlated 2π exchange is derived from the quasiempirical result provided by Ref. [14]. In the short-dashed line, the correlated 2π exchange is replaced by sharp mass σ' and ρ exchange as used in the (full) Bonn potential [10]. The error bars are taken from the empirical analysis of Bugg [25] (triangles) and Arndt *et al.* [26] (circles). The dotted lines denote the π-exchange contribution only while the dash-double-dotted lines arise from $\pi + \omega$ exchange. Finally, for the dash-dotted curve, uncorrelated 2π exchange is added to $\pi + \omega$. All calculations are done in the K-matrix approximation.

from the quasiempirical $N\bar{N} \to 2\pi$ amplitudes [14], and (iii) sharp σ' and ρ exchange as used in the Bonn potential. As described before, single $\pi + \omega$ exchange and the uncorrelated 2π exchange (Fig. 1) are exactly the same for all these cases.

Since we are dealing here with high partial waves, the results are essentially dictated by the behavior of the models in the scalar channel, which provides the longer-range contribution. As expected from the foregoing results concerning the (on-shell) potentials (Fig. 9), the dynamical model provides slightly more attraction than the quasiempirical result in all partial waves. However—as we pointed out before—the difference is quite small, despite the relatively large discrepancy in the scalar spectral functions.

On the other hand, σ' $(+\rho)$ exchange provides substantially less attraction in some partial waves—again to be anticipated from the potential results. Those partial waves in which the discrepancy is small are dominated by one-pion exchange anyway. We have split up the potential into the various terms in order to really show that a realistic description of correlated 2π exchange provides a contribution which is considerably larger compared to the Bonn parametrization, by an amount increasing with the angular momentum of the partial wave. Furthermore, our results strengthen the role of the correlated 2π contribution compared to the uncorrelated part even more.

For the $^1G_4$ partial wave, the increased attraction aris-

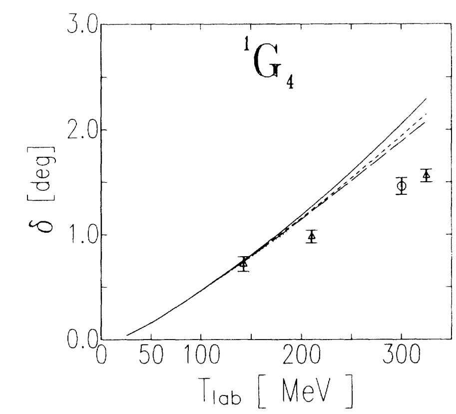

FIG. 13. *np* phase shifts in the $^1G_4$ partial wave, as a function of the nucleon laboratory kinetic energy, predicted by our dynamical model for correlated 2π exchange, supplemented by π exchange and ω exchange ($g^2_{NN\omega}/4\pi = 5.7$) and the uncorrelated 2π-exchange contributions as calculated in the Bonn potential [10], using $g^2_{NN\pi}/4\pi = 14.4$ (solid line). The dashed line arises if ω exchange is increased by using $g^2_{NN\omega}/4\pi = 20$. For the dash-dotted line, uncorrelated contributions arising from $\pi\rho$ exchange, as calculated in the Bonn potential [10], are added to the interaction leading to the dashed line. The dotted line is obtained by using soft πNN and $\pi N\Delta$ form factors, $\Lambda_{NN\pi} = \Lambda_{N\Delta\pi} = 0.8$ GeV, instead of $\Lambda_{NN\pi}(\Lambda_{N\Delta\pi}) = 1.3(1.2)$ GeV, in the interaction leading to the dash-dotted line, both in the one-pion-exchange potential and in the uncorrelated 2π-exchange contributions. The error bars are taken from the empirical analysis of Bugg [25] (triangles) and Arndt *et al.* [26] (circles) .

ing from the realistic description of correlated 2π exchange now leads to a definite discrepancy compared to the empirical information: already at medium energies the empirical phase shifts are definitely lower. Of course, the present model is not complete. In the full Bonn model, ω exchange is considerably larger and (uncorrelated) $\pi\rho$ exchange is included, both of which bring the phase shifts down somewhat. However, due to the short range of these contributions, the shift is very small in this $L = 4$ partial wave, as demonstrated in Fig. 13, and by no means sufficient to bring the phase shifts into agreement with experiment. Note also that a full calculation (instead of the K-matrix approximation done here) will not change the results noticeably. We have checked for the full Bonn potential that the K-matrix approximation is extremely good in this partial wave. Consequently, the discrepancy essentially survives in a more complete calculation.

What remains to bring the phase shifts down is a reduction of the one-pion-exchange contribution. The first idea which comes to mind is to make the πNN form factor softer. Indeed, a considerable body of information suggests that the πNN form factor is quite soft, characterized by a value of 0.8 GeV for the monopole cutoff mass. However, as also shown in Fig. 13, the phase shifts barely change even if we take $\Lambda = 0.8$ GeV for both πNN and $\pi N\Delta$ vertices. This is not surprising since high angular momentum partial waves ($L \geq 4$) are known to be essentially independent of form factor modifications. This fact shows once more the advantage of concentrating the efforts on high partial waves, since one is here essentially free of ambiguities due to form factors and the short-range part of the interaction.

The only possibility to get a noticeable reduction of the ${}^1G_4$ phase shifts is to reduce the πNN coupling constant. Indeed, the Nijmegen group has claimed for quite some time that not only $g^2_{pp\pi_0}$ [22] but also $g^2_{np\pi^+}$ (of relevance here) should be substantially smaller ($g^2_{np\pi^+}/4\pi \approx 13.5$ [23]) compared with the value $g^2_{np\pi^+}/4\pi = 14.4$ established before. A comparably lower value has been obtained in a recent phase shift analysis done by the VPI group [24]. Although there is still a vigorous debate over this subject, we take, in a second step, the lower value $g^2_{NN\pi}/4\pi = 13.5$ everywhere, i.e., in the one-pion-exchange potential (OPEP), in the uncorrelated $2\pi + \pi\rho$-exchange piece, and in our dynamical model for correlated 2π exchange. (Note that, for this calculation, we do not readjust our $N\bar{N} \to \pi\pi$ amplitudes to the quasiempirical result since the latter is based on the former value of $g^2_{NN\pi}$ and is thus expected to change also if $g^2_{NN\pi}$ is reduced. In any case, the change is expected to be smaller than the overall uncertainty of the quasiempirical result.) Results (now with $g^2_{NN\omega}/4\pi = 20$) are compared with the corresponding calculation using everywhere $g^2_{NN\pi}/4\pi = 14.4$ in Fig. 14. Obviously, this change provides a substantial reduction, mainly due to the modification of OPEP, which dominates the interaction in these high partial waves. For ${}^1G_4$, however, it is not sufficient to bring the phase shifts in agreement with the empirical result. This is not necessarily an indication for a still lower coupling constant since the phase shift

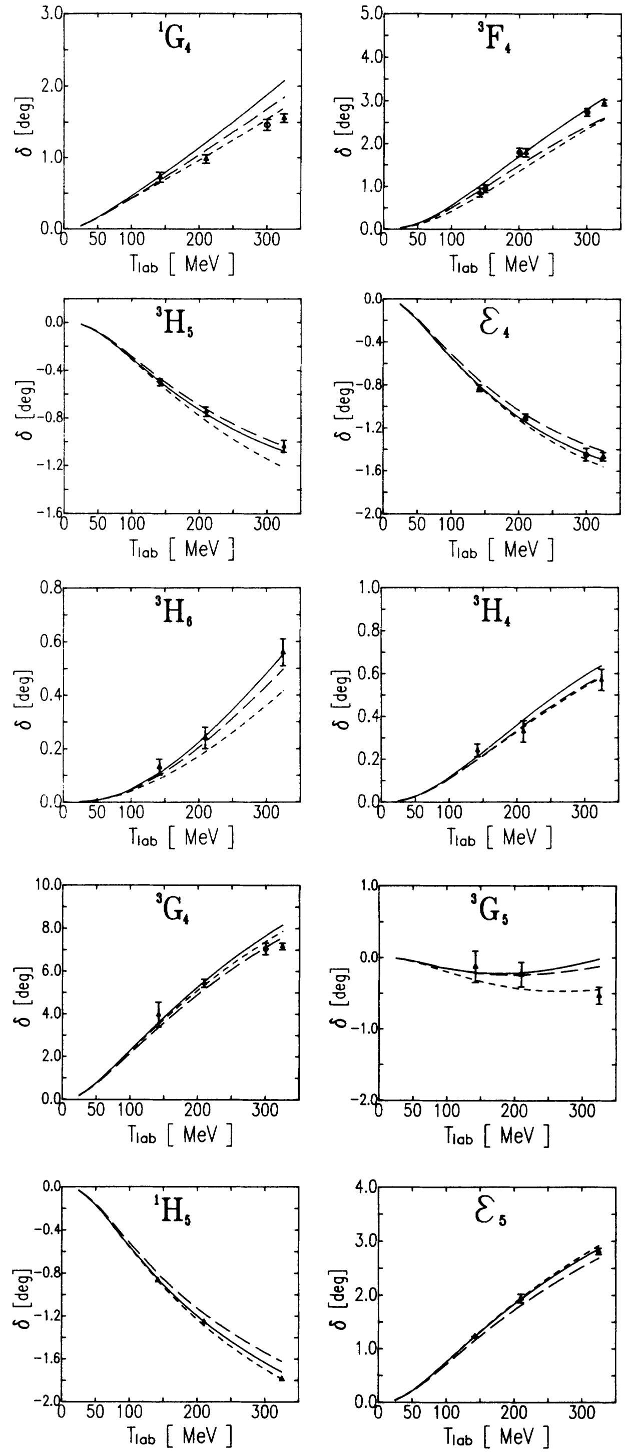

FIG. 14. np phase shifts as function of the nucleon laboratory kinetic energy, predicted by our dynamical model for correlated 2π exchange, supplemented by π exchange and ω exchange ($g^2_{NN\omega}/4\pi = 20$) and the uncorrelated 2π as well as $\pi\rho$ contributions as calculated in the Bonn potential [10], with $g^2_{NN\pi}/4\pi = 14.4$ (13.5) for the solid (long-dashed) line. The short-dashed line is based on the same interaction as the solid line, with the correlated 2π-exchange contribution replaced by (sharp mass) σ' and ρ exchange as used in the full Bonn potential [10]. The error bars are taken from the empirical analysis of Bugg [25] (triangles) and Arndt *et al.* [26] (circles).

analysis of Ref. [25] has the constraint $g^2_{np\pi^+}/4\pi = 14.3$ and is thus expected to change somewhat if the lower value would be taken as a constraint.

Consequently, if we avoid arbitrarily adjusting the intermediate-range attraction but make use of the constraints given by a realistic evaluation of correlated 2π exchange the resulting NN interaction seems to prefer a somewhat smaller πNN coupling constant. Of course lower NN partial waves, and especially NN observables, will have to be investigated in order to confirm this statement. Nevertheless, we feel that our results, being independent of assumptions about short-range dynamics, provide additional support for the need to redetermine $g^2_{NN\pi}$ from πN data.

IV. SUMMARY AND OUTLOOK

In this paper, we have developed a dynamical model for the NN interaction arising from correlated 2π exchange in the scalar and vector channel. Starting point was a microscopic model for the $N\bar{N} \to \pi\pi$ process based on nucleon as well as Δ-isobar exchange, together with a $\pi\pi$ interaction which has been likewise derived in the meson exchange framework and describes $\pi\pi$ scattering data sufficiently from threshold to about 1.3 GeV c.m. energy. In the pseudophysical region the resulting $N\bar{N} \to \pi\pi$ amplitudes are compared with those obtained by Höhler and Pietarinen by analytic continuation of empirical πN and $\pi\pi$ data. Although some discrepancies occur in the scalar channel, these have only a minor effect on the correlated 2π-exchange interaction, which we have obtained from the $N\bar{N} \to \pi\pi$ amplitudes via a dispersion integral over the unitarity cut, subtracting the uncorrelated part.

It turned out that the results differed considerably from the simple parametrization in terms of (sharp mass) σ' and ρ exchange as used in the full Bonn NN potential. In the scalar channel the σ' exchange strongly underestimates the contribution in high partial waves; in the vector channel the ρ exchange of the Bonn potential is likewise much weaker due to the use of a phenomenological form factor which significantly cuts down the contribution in the physical region.

We have investigated the effect of these modifications in high angular momentum NN scattering phase shifts. Throughout, there is a pronounced upward shift compared to the former Bonn results, which mainly arises from the increased attraction generated by correlated 2π exchange in the scalar channel. In some cases, it leads to definite discrepancies with empirical phase shifts, which can be reduced by lowering the πNN coupling constant in accordance with findings of the Nijmegen and VPI groups.

Whether the improved treatment of correlated 2π exchange really requires a lower πNN coupling constant can of course only be decided (if at all) by also looking at the consequences for low partial waves and, ultimately, for the NN observables. Here, the Born approximation is not valid anymore; therefore, a suitable off-shell extrapolation of the correlated 2π-exchange potential is required. Also, $\pi\rho$-exchange processes contained in the Bonn model, which are not very relevant in high partial waves, become important in low partial waves and require a consistent treatment of ρ exchange. Corresponding investigations are under way.

With this dynamical model for correlated 2π exchange it is possible to discuss medium modifications in a well-defined way. First calculations (based on a slightly different model) have already been performed and provided interesting results [15].

Finally, it should come as no surprise that such an improved treatment of correlated 2π exchange also has considerable impact in other hadronic reactions. So far, we have looked at the πN [27] and KN [28] systems. A corresponding investigation for the hyperon-nucleon $(\Lambda N, \Sigma N)$ system is under way.

Thanks are due to J. Haidenbauer for useful discussions and assistance in obtaining some numerical results.

[1] H. Yukawa, Proc. Phys. Math. Soc. Jpn. **17**, 48 (1935).
[2] K. Erkelenz, Phys. Rep. C **13**, 191 (1974).
[3] R. de Tourreil, B. Rouben, and D.W.L. Sprung, Nucl. Phys. **A242**, 445 (1975).
[4] M.M. Nagels, T.A. Rijken, and J.J. de Swart, Phys. Rev. D **17**, 768 (1978).
[5] A.D. Jackson, D.O. Riska, and B. VerWest, Nucl. Phys. **A249**, 397 (1975).
[6] G.E. Brown and A.D. Jackson, *Nucleon-Nucleon Interaction* (North-Holland, Amsterdam, 1979), p. 151.
[7] M. Lacombe, B. Loiseau, J.-M. Richard, R. Vinh Mau, P. Pirès, and R. de Tourreil, Phys. Rev. C **12**, 1495 (1975).
[8] R. Vinh Mau, in *Mesons in Nuclei*, edited by M. Rho and D.H. Wilkinson (North-Holland, Amsterdam, 1979), Vol. 1, p. 151.
[9] M. Lacombe, B. Loiseau, J.-M. Richard, R. Vinh Mau, J. Côté, P. Pirès, and R. de Tourreil, Phys. Rev. C **21**, 861 (1980).
[10] R. Machleidt, K. Holinde, and Ch. Elster, Phys. Rep. **149**, 1 (1987).
[11] J.W. Durso, A.D. Jackson and B.J. VerWest, Nucl. Phys. **A345**, 471 (1980).
[12] D. Lohse, J.W. Durso, K. Holinde, and J. Speth, Nucl. Phys. **A516**, 513 (1990).
[13] T. Hatsuda and S.H. Lee, Phys. Rev C **41**, R34 (1992).
[14] G. Höhler, F. Kaiser, R. Koch, and E. Pietarinen, *Handbook of Pion-Nucleon Scattering*, Physics Data 12-1 (Fachinformationszentrum, Karlsruhe, 1979).
[15] J.W. Durso, H.-C. Kim, and J. Wambach, Phys. Lett. B **298**, 267 (1993).
[16] D. Amati, E. Leader, and B. Vitale, Nuovo Cimento **17**, 68 (1960); W. Lin and B.D. Serot, Nucl. Phys. **A512**, 637 (1990).
[17] W.R. Frazer and J.R. Fulco, Phys. Rev. **117**, 1603 (1960).
[18] Th. Hippchen, J. Haidenbauer, K. Holinde, and V. Mull, Phys. Rev. C **44**, 1323 (1991).
[19] V. Mull, J. Haidenbauer, Th. Hippchen, and K. Holinde, Phys. Rev. C **44**, 1337 (1991).
[20] G. Höhler and E. Pietarinen, Nucl. Phys. **B95**, 210 (1975).

[21] J. Haidenbauer, K. Holinde, and M.B. Johnson, Phys. Rev. C **48**, 2190 (1993).
[22] J.R. Bergervoet, P.C. van Campen, R.A.M. Klomp, J.-L. de Kok, T.A. Rijken, V.G.J. Stoks, and J.J. de Swart, Phys. Rev. C **41**, 1435 (1990).
[23] R.A.M. Klomp, V.G.J. Stoks, and J.J. de Swart, Phys. Rev. C **44**, R1258 (1991).
[24] R.A. Arndt, Z. Li, L.D. Roper, and R.L. Workman, Phys. Rev. Lett. **65**, 157 (1990).
[25] D.V. Bugg, Phys. Rev. C **41**, 2708 (1990).
[26] R.A. Arndt, J.S. Hyslop III, and L.D. Roper, Phys. Rev. D **35**, 128 (1987).
[27] C. Schütz, J.W. Durso, K. Holinde, and J. Speth, Phys. Rev. C **49**, 2671 (1994).
[28] M. Hoffmann, J.W. Durso, K. Holinde, and J. Speth (unpublished).